Meta Distribution of the SIR in Moving Networks

Xiaoxuan Tang, Xiaodong Xu, *Senior Member, IEEE,* and Martin Haenggi, *Fellow, IEEE*

***Abstract*—Moving networks (MNs) with moving base stations (BSs) provide ubiquitous and constant services to cellular devices/user equipment (UEs) in 5-th generation systems. Moving BSs are mounted on top of vehicles. To describe the randomness of the BSs, a tractable stochastic geometry model for MNs is proposed. A definition of the conditional success probability and meta distribution (MD) of the signal-to-interference ratio (SIR) for MNs is proposed. The MD is used to assess the benefits of MNs. In single-tier MNs with high mobility, we determine the moments of the conditional success probability given the point process for the calculation of the MD and the mean local delay. The results show that the mean local delay is finite and the variance is reduced to 0. A closed-form approximation of the variance is proposed for general mobility levels. Using the approximated variance, we propose a beta approximation of the MD. The single-tier model is then extended to a two-tier heterogeneous MN model. Tractable expressions of the mean success probability and the variance for both the overall network and the typical UE in each tier are obtained. They reveal that moving BSs can reduce the variance among UEs while keeping the mean success probability constant.**

***Index Terms*—Moving network, stochastic geometry, Poisson point process, meta distribution, SIR, mean local delay, coverage probability, heterogeneous cellular networks.**

I. Introduction

A. Motivation

Proposed by the European 5-th Generation (5G) project Mobile and Wireless Communications Enablers for the Twenty-twenty Information Society (METIS), the moving network (MN) is a promising solution to provide ubiquitous and constant services to cellular devices/user equipment (UEs) in 5G scenarios [1]. In MNs, moving base stations (BSs) are deployed on top of vehicles (buses, trams, etc.). Motivated by antenna design constraints, the outdoor antenna system of the moving BS is assumed to be optimized for the moving backhaul link to receive/transmit signals from/to macro BSs, and intravehicular antennas are used for the UEs. The half-duplex moving BSs are considered to have similar functionality as the fixed BSs standardized in Long-Term Evolution (LTE). The 3rd generation partnership project (3GPP) clarifies that the moving BSs can exploit various smart antenna techniques and advanced signal processing schemes for their device size, available power, number of antennae, etc. [2]. A dense deployment of moving BSs in MNs provides a significant number of moving access points for UEs. This flexible network architecture greatly changes conventional cellular networks.

This work is supported by National Natural Science Foundation of China No. 61871045 and 111 Project of China B16006.

X. Tang is with the China Mobile Research Institute, Beijing, 100053, China. (email: tangxiaoxuan@chinamobile.com)

X. Xu is with the National Engineering Laboratory for Mobile Networks, Beijing University of Posts and Telecommunications, Beijing, 100876, China. (Corresponding author, email: xuxiaodong@bupt.edu.cn)

M. Haenggi is with the Department of Electrical Engineering, University of Notre Dame, Notre Dame, IN 46556, USA. (email: mhaenggi@nd.edu)

To assess the potential benefits of integrating moving BSs in heterogeneous cellular networks (HCNs), the signal-to-interference ratio (SIR) distribution plays a key role in evaluating the downlink performance, especially in interference-limited networks. Stochastic geometry has been widely used as an analytical approach to model and quantify the SIR distribution in wireless networks [3]. It provides tools and models like the Poisson point process (PPP) to describe the randomness of node deployment quite accurately [4] and obtain insightful theoretical results, especially in dense cellular networks [5].

The conventional performance analysis for networks modeled by a point process Φ focuses on the complementary cumulative distribution (ccdf) of the SIR. The ccdf of the SIR of the typical UE is interpreted as the standard (mean) transmission success probability $p_{\rm s}(\theta) \triangleq \mathbb{P}(\mathrm{SIR} > \theta)$. While this average metric answers the question "What fraction of UEs in a Poisson cellular network succeed in transmitting given an SIR threshold θ?", it does not reveal any information on the reliabilities of individual links/UEs.

B. Meta Distribution

Recently, the meta distribution (MD) of the SIR has been introduced as a performance metric that provides complete *spatial distributions* rather than merely *spatial averages*. The MD has been evaluated in both Poisson bipolar networks and downlink cellular networks [6]. It is the distribution (ccdf) of the conditional success probability $P_{\rm s}(\theta)$. $P_{\rm s}(\theta)$ is the probability that the SIR at the origin exceeds threshold θ given the BS process. The MD of the SIR is a two-parameter distribution function defined as [6]

$$F(x) \triangleq \bar{F}(\theta, x) = \mathbb{P}(P_{\rm s}(\theta) > x),\ \theta \in \mathbb{R}^+, x \in [0,1], \quad (1)$$

where x refers to the reliability. The conditional success probability is defined as $P_{\rm s}(\theta) \triangleq \mathbb{P}(\mathrm{SIR} > \theta \mid \Phi)$, given a stationary point process Φ and averaging out the fading. The random variable $P_{\rm s}(\theta)$ describes the success probability of the link between a user at the origin and its serving BS. For ergodic point processes Φ, the MD gives the fraction of links or users that can achieve an SIR of θ with reliability at least x. Unlike the standard success probability, the MD answers some key questions operators have, such as: "What is the fraction of UEs in a cellular network achieve 90% link reliability given an SIR threshold θ?" or "How will the mobility in MNs affect the link reliability distribution among UEs?".

Since it seems infeasible to derive the meta distribution directly, we focus on the b-th moments of the conditional success probability, defined as

$$M_b(\theta) \triangleq \mathbb{E}(P_{\mathrm{s}}(\theta)^b). \tag{2}$$

For the standard success probability, we have $p_{\mathrm{s}}(\theta) \equiv M_1 \triangleq \mathbb{P}(\mathrm{SIR} > \theta)$, i.e., the first moment of the conditional success probability is the average transmission success probability of the network. The variance of the conditional success probability is another key performance metric, given by $\mathrm{var}(P_{\mathrm{s}}) = M_2 - M_1^2$. It quantifies the differences among the UEs, i.e., the fairness of the network.

C. Related Work

Moving Networks in the METIS project refers to novel concepts that focus on moving network nodes/terminals. Moving nodes provide better propagation conditions with less shadowing and path loss [7]. The vehicular penetration loss (VPL) can be 25-30 dB and more for frequencies above 6 GHz when radio signals are transmitted through the hull of a vehicle [8]. Proper antenna deployment circumvents the VPL and reduces the interference from moving BSs to UEs outside the vehicle. Compared with fixed-relay transmission and direct transmission, moving nodes enhance the performance for vehicular UEs in a single-cell system [9]. It is shown in [10] that moving BS transmission still outperforms transmission assisted by a fixed relay as well as direct transmission based on a two cell system model. By using a hexagonal grid model for the moving BSs, researchers came to the conclusion that moving BSs can improve the coverage probability of both boundary extravehicular UEs and vehicular UEs [11]. However, the dense deployment of moving BSs greatly changes the architecture of cellular networks. The conventional network models like the hexagonal grid model and the single cell model are oversimplified and ignore the irregularity of MNs.

With models like the PPP, stochastic geometry captures the randomness of node deployment. It has been applied in a growing number of studies such as the analysis of the cross-tier handover in heterogeneous networks [12], throughput for full-duplex wireless networks [13], and coordinated multipoint joint transmission in heterogeneous networks [14]. With regard to the MNs, researchers proposed basic analytical models for MNs by utilizing stochastic geometry to obtain mathematical expressions [15]–[18]. The temporal correlation of the outage is analyzed for the design of new retransmission schemes with correlation-awareness in mobile network [19]. These works related to the SIR analysis in MNs only focus on the mean success probability $p_{\mathrm{s}}(\theta)$ or outage probability, not on the MD.

To the best of our knowledge, the MD can not be calculated directly. With the known moments of P_{s}, the exact MD can be calculated by the Gil-Pelaez theorem by tedious numerical integration of the imaginary moments. The numerical integration requires a careful selection of the range and step size. The beta distribution is shown to be an efficient approximation to the MD by matching its first and second moments [6]. This method yields good results if the actual distribution is close to a beta distribution. Very recently, research on the calculation of the MD led to new approaches. The work [20] reconstructs the MD from its moments using Fourier-Jacobi expansion. This method uses the information contained in the higher moments resulting in a better accuracy than the beta approximation, but its convergence properties are unknown. Given that we already have the moments of P_{s}, an efficient method based on binomial mixtures is more promising for its simplicity and uniform convergence properties [21]. It is based on a simple linear transform of the moments of P_{s}.

Recently, the MD has been extended to more scenarios [6], [22]–[29]. The paper on the MD [6] firstly obtained an analytical expression for the exact MD and a closed-form expression of the moments M_b of the conditional success probability for both Poisson bipolar and cellular networks with Rayleigh fading. The MD concept is also applied in the performance evaluation of mm-wave device-to-device (D2D) networks [22], the cellular network uplink and downlink with fractional power control [23], the secrecy rate for a legitimate link in the presence of eavesdroppers [24], Poisson networks with interference cancellation at the receivers [25] and D2D underlaid cellular networks [26]. Besides, an SIR MD analysis is conducted for the homogeneous independent Poisson (HIP) downlink model with biasing factors [27]. An MD analysis for MNs is an open issue. Conventional cellular networks with static transmitters can be considered as a special case of the MNs by setting the speed to zero.

D. Contribution

We obtain the SIR MD for MNs and analyze a series of key performance metrics. In MNs, the meta distributions for the extreme cases with zero and infinite mobility are derived, while the intermediate range of mobility is evaluated by simulations, and tight approximations are obtained. The main contributions of this paper are the following:

- We propose definitions of the conditional success probability and the MD for moving networks.
- For single-tier MNs with high mobility (speeds tending to infinity), we show that the conditional success probabilities degenerate to a deterministic quantity, i.e., the variance tends to 0 and the MD to a step function.
- For single-tier MNs with general speed, a closed-form approximation of the variance is given. To justify the approximation, we show by simulation that the interference-to-signal ratios of a PPP before and after displacing the points by twice the mean nearest-neighbor distance are essentially uncorrelated. Using the approximated variance, we propose a beta approximation of the MD for general speeds.
- We extend the single-tier model to two-tier heterogeneous MNs. For the conditional high-mobility case in two-tier MNs, we derive the standard success probability M_1 and the variance $M_2 - M_1^2$ for both the overall network and the typical UE in each tier give that the serving BS from tier 2 is fixed.
- From the theoretical and simulation results, we gain insights on the benefits of MNs and the impact of other network parameters like the density ratio, transmission

power, and bias factor. An important conclusion is that mobility mitigates the high variance brought by offloading UEs from macro BSs while maintaining roughly the same standard success probability.

Notations: The mean of the random variable X is denoted by $\mathbb{E}[X]$. The probability of event A is denoted by $\mathbb{P}[A]$. The Gaussian hypergeometric function is denoted by ${}_2F_1(.,.;.;.)$. The main symbols employed in this paper are explained in Table I.

TABLE I
LIST OF SYMBOLS

Symbol	Definition
$\Phi_i(t)$	PPP to constitute the i-th tier
$\lambda_i(t)$	Intensity of BSs in the i-th tier
P_i	Transmission power of BSs in tier i
α	Path loss exponent
θ	SIR threshold for success transmission
β_i	Range expansion bias for the i-th tier
v	Speed of MBSs
$p_{(i)\mid r_i(t)}$	Conditional access probability for tier i given $r_i(t)$
$p_{(i)}$	Access probability for tier i
$P_{\rm s}^{[v]}(\theta)$	Conditional success probability for MNs with speed v
$P_{{\rm s}\mid(i)}^{[v]}(\theta)$	Conditional success probability conditioned on tier i serving the user
$P_{{\rm s}\mid(i),r_i(t)}^{[v]}(\theta)$	Conditional success probability conditioned on tier i serving the user given $r_i(t)$
$M_b^{[v]}$	b-th moment of $P_{\rm s}^{[v]}(\theta)$ for MNs with speed v
$M_{b,(i)}^{[v]}$	b-th moment of $P_{\rm s}^{[v]}(\theta)$ for tier i
$M_{b\mid(i)}^{[v]}$	b-th moment of $P_{\rm s}^{[v]}(\theta)$ conditioned on tier i serving the user
$M_{b,(2)}'^{[\infty]}$	b-th moment for tier 2 given that the serving BS is at distance r_2
$M_b'^{[\infty]}$	b-th moment for MNs given that the serving moving BS is at distance r_2
$V^{[v]}$	Variance of $P_{\rm s}^{[v]}(\theta)$ for MNs with speed v
$V_{\mid(i)}^{[v]}$	Variance of $P_{\rm s}^{[v]}(\theta)$ for tier i
$V'^{[v]}$	Variance of $P_{\rm s}^{[v]}(\theta)$ for MNs given that the serving BS is at distance r_2
$V_{\mid(i)}'^{[v]}$	Variance of $P_{\rm s}^{[v]}(\theta)$ for tier i given that the serving BS is at distance r_2

II. Single-tier moving networks

A. System Model

A single-tier cellular network with mobility is considered to analyze the effect of mobility. We assume the standard path loss law with path loss exponent $\alpha = 2/\delta > 2$ and Rayleigh fading h. At time t, BSs form a point process $\Phi(t) \triangleq \{x \in \Phi_0 : x + \boldsymbol{v}_x t\}, t \in \mathbb{R}$, where Φ_0 is a PPP of intensity λ. The velocity vector $\boldsymbol{v}_x$ of each point x is random and i.i.d. for all x with identical speed $\|\boldsymbol{v}_x\| = v$ and random movement direction uniformly distributed in $[0, 2\pi)$. Accordingly, $\Phi(t)$ is a homogeneous PPP at each time t with constant intensity λ. Besides, we suppose that each BS uses an identical transmission power P and is active at all times. The two extreme cases of mobility are the high-mobility case, where $v \to \infty$, and the static case $v = 0$, where the BSs stay fixed forever. The single-tier static network (SN) is a special case of this model by setting $v = 0$, resulting in $\Phi(t) \equiv \Phi_0$. The downlink association scheme is the nearest-BS scheme, i.e., the typical UE at the origin is served by its nearest BS $x_0(t) = \arg\min\{x \in \Phi(t) : \|x\|\}$. The distance from the serving BS to the typical UE located at the origin is $r(t) = \|x_0(t)\|$.

The SIR of the typical UE assumed to be located at the origin can be written as

$$\mathrm{SIR}(t) = \frac{P h_{x_0(t)} r(t)^{-\alpha}}{\sum\limits_{x(t)\in\Phi(t)\setminus\{x_0(t)\}} P h_{x(t)} \|x(t)\|^{-\alpha}}. \tag{3}$$

where $h_{x(t)}$ denotes the Rayleigh fading between the typical user at the origin and the BS at $x(t)$, $h_{x(t)}$ is exponential with mean 1 and i.i.d. for all points in the PPP and over time.

With increasing speed, the frequency of handovers from one BS to another one increases. While the impact of such handovers is beyond the scope of this paper, we note that handovers in moving networks are easier to handle than handovers in systems with maximum instantaneous-SIR BS association, which is considered, e.g., in [30]. This is due to the following two reasons: First, in moving networks, it is predictable when another BS becomes the nearest one, since the locations and directions of the mobile BSs can be assumed known. Second, only users near the (moving) cell edge are candidates for handoffs. In contrast, with maximum instantaneous-SIR BS association, handovers can occur at any user at any time, due to the rapid variations of the small-scale fading, and they are impossible to predict. In addition, there are many candidate BS that could become the serving one, i.e., the handover mechanism needs to select from many.

B. Definition of the SIR MD in Moving Networks

The conditional success probability $P_{\rm s}(\theta)$ can be viewed as the temporal average over a certain number of coherence times. In SNs, the averaging over the fading while conditioning on BS point process Φ corresponds to a separation of temporal and spatial scales. If the BSs are moving, the averaging also includes the different BS locations over a time period. This way, the concept of the MD can be extended to the case with mobility. Here, we formally introduce the definition of the conditional success probability for MNs.

Definition 1 (Conditional success probability for MNs) *The conditional success probability for MNs is defined as*

$$\begin{aligned} P_{\rm s}^{[v]}(\theta) &\triangleq \int_0^1 \mathbb{E}_h \mathbb{1}\left(\mathrm{SIR}(t) > \theta\right) \mathrm{d}t \\ &= \int_0^1 \mathbb{P}(\mathrm{SIR}(t) > \theta \mid \Phi(t)) \mathrm{d}t, \end{aligned} \tag{4}$$

where $\mathbb{1}(\cdot)$ is the indicator function.

The characteristic function of $X \triangleq \log P_{\rm s}^{[v]}(\theta)$ is $\varphi_X(u) \triangleq \mathbb{E}e^{juX} = M_{ju}$, $j \triangleq \sqrt{-1}$, $t \in \mathbb{R}$. The meta distribution can be obtained from the Gil-Pelaez theorem [31] with the purely imaginary moments M_{ju} as

$$\bar{F}(\theta, x) = \frac{1}{2} + \frac{1}{\pi}\int_0^\infty \frac{\Im[e^{-ju\log x} M_{ju}]}{u} \mathrm{d}u, \tag{5}$$

where $\Im(z)$ denotes the imaginary part of the complex number z. With the moments M_b in hand, the meta distribution can be calculated for each value of x and θ.

C. Spatial Correlation of the Interference-to-Signal Ratio

The definition of the interference-to-average-signal ratio $\bar{\mathsf{ISR}}$ is first given in [32] as

$$\bar{\mathsf{ISR}} \triangleq \frac{I}{\mathbb{E}_h(S)} = \frac{\sum\limits_{x\in\Phi\setminus\{x_0\}} h_x \|x\|^{-\alpha}}{\|x_0\|^{-\alpha}}, \tag{6}$$

where I is the sum power of all interferers and $\bar{S} = \mathbb{E}_h(S)$ is the signal power averaged over the fading. Its mean follows as $\mathsf{MISR} \triangleq \mathbb{E}\left(\|x_0\|^\alpha \cdot \sum\limits_{x\in\Phi\setminus\{x_0\}} \|x\|^{-\alpha}\right)$, and the success probability under Rayleigh fading can be expressed as the Laplace transform of the $\bar{\mathsf{ISR}}$ as

$$p_s(\theta) = \mathbb{P}(h > \theta\, \bar{\mathsf{ISR}}) = \mathbb{E}\left[\exp(-\theta\, \bar{\mathsf{ISR}})\right]. \tag{7}$$

The $\bar{\mathsf{ISR}}$ includes fading in the interferers' channels. Since the fading affects the spatial correlation, here we focus on a version of the ISR that does not include fading, i.e., the conditional mean $\bar{\mathsf{ISR}}$ given the point process. This way, our findings are more general and robust as they not depend on a particular fading model.

We set $v = 1$ and let ISR_Δ be the conditional mean interference-to-signal ratio in $\Phi(\Delta)$, *i.e.*, after displacing each point by Δ in a random direction:

$$\mathsf{ISR}_\Delta \triangleq \|x_0(\Delta)\|^\alpha \sum_{x\in\Phi(\Delta)\setminus\{x_0(\Delta)\}} \|x\|^{-\alpha}.$$

Remark. *The* $(\mathsf{ISR}_\Delta)_{\Delta\in\mathbb{R}}$ *are identically distributed since* $\Phi(t)$ *is a PPP at all times.*

Since ISR is a function of the distance ratio between the serving and interfering BSs, $\exp(-\theta\,\mathsf{ISR})$ is a good quantity to measure the spatial correlation in the success probability. An analytical derivation of $\mathbb{E}(e^{-\theta\,\mathsf{ISR}_0} e^{-\theta\,\mathsf{ISR}_\Delta})$ seems impossible, since this functional falls outside the classes of functionals for which exact expressions exist. Instead, we resort to an approximation that is based on the following intuition: Upon displacing each point by twice the mean nearest-neighbor distance, the neighborhood around the origin changes drastically, thus we can expect the correlation in the ISR to essentially drop to zero.

Claim. *In a PPP with intensity* $\lambda = 1$, ISR_0 *and* ISR_1 *are essentially uncorrelated. More precisely, the linear correlation coefficient of* $\exp(-\theta\,\mathsf{ISR}_0)$ *and* $\exp(-\theta\,\mathsf{ISR}_1)$ *is below 0.05 for* $\alpha \geq 3$ *and all* θ.

To support this claim, simulations have been carried out to explore the correlation of ISR_0 and ISR_Δ. Figs 1(a) and 1(b) show the correlation between $e^{-\theta\,\mathsf{ISR}_0}$ and $e^{-\theta\,\mathsf{ISR}_\Delta}$ as a function of Δ for different values of θ and the correlation between ISR_0 and ISR_Δ (dashed curve) for $\alpha = 4$ and $\alpha = 3$, respectively. It is apparent that for $\theta = -10$ dB, the correlation between $e^{-\theta\,\mathsf{ISR}_0}$ and $e^{-\theta\,\mathsf{ISR}_\Delta}$ is essentially the same as the correlation of ISR_0 and ISR_Δ. Also, the coherence length gets smaller as θ increases.

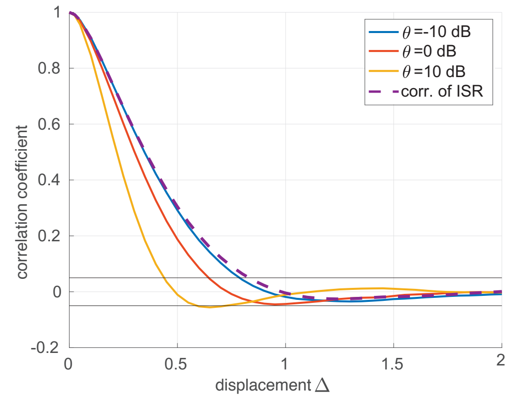

(a) $\alpha = 4$

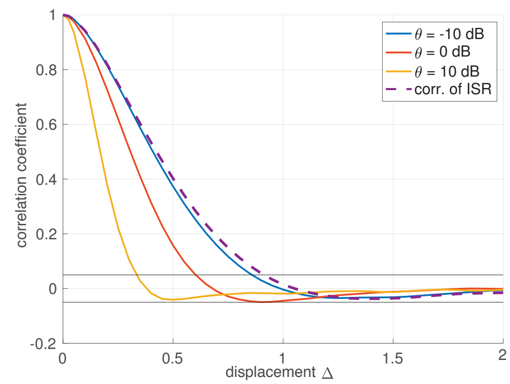

(b) $\alpha = 3$

Fig. 1. Correlation of $\exp(-\theta\,\mathsf{ISR}_0)$ and $\exp(-\theta\,\mathsf{ISR}_\Delta)$ where $\lambda = 1$. The horizontal lines are drawn at $|\rho| = 0.05$.

Remarks:

- *Let* $\rho(X,Y) = \mathrm{cov}(X,Y)/\sqrt{\mathrm{var}(X)\,\mathrm{var}(Y)}$ *be the linear correlation coefficient between the random variables* X *and* Y*. As* $\theta \to 0$*, the correlation between* $e^{-\theta\,\mathsf{ISR}_0}$ *and* $e^{-\theta\,\mathsf{ISR}_\Delta}$ *approaches the correlation of* ISR_0 *and* ISR_Δ*, i.e.,*

$$\rho(e^{-\theta\,\mathsf{ISR}_0}, e^{-\theta\,\mathsf{ISR}_\Delta}) \sim \rho(\mathsf{ISR}_0, \mathsf{ISR}_\Delta), \quad \theta \to 0.$$

The convergence happens fast, since, as $\theta \to 0$,

$$\mathrm{cov}(e^{-\theta\,\mathsf{ISR}_0}, e^{-\theta\,\mathsf{ISR}_\Delta}) \sim \theta^2$$

and (naturally, for the above to hold)

$$\sqrt{\mathrm{var}(e^{-\theta\,\mathsf{ISR}_0})\,\mathrm{var}(e^{-\theta\,\mathsf{ISR}_\Delta})} = \mathrm{var}(e^{-\theta\,\mathsf{ISR}_0}) \sim \theta^2.$$

This is easy to show from the expansion $e^{-x} \sim 1 - x + x^2/2$.

- *The correlation of* ISR_0 *and* ISR_Δ *can be written as*

$$\rho(\mathsf{ISR}_0, \mathsf{ISR}_\Delta) = \frac{\mathbb{E}(\mathsf{ISR}_0\,\mathsf{ISR}_\Delta) - \mathsf{MISR}^2}{\mathrm{var}(\mathsf{ISR})}. \tag{8}$$

The variance is

$$\mathrm{var}(\mathsf{ISR}) = \mathbb{E}(\mathsf{ISR}^2) - \mathsf{MISR}^2 = \frac{\delta}{2-\delta}.$$

This follows from Theorem 2 in [33], which states that

$$\mathsf{MISR} = \mathbb{E}(\mathsf{ISR}_0) = \frac{\delta}{1-\delta}, \quad \mathbb{E}(\mathsf{ISR}_0^2) = \frac{\delta}{(1-\delta)^2(2-\delta)}.$$

So the only unknown quantity in (8) *is the expectation of the product of* ISR_0 *and* ISR_Δ*, which is an affine function of* ρ*:*

$$\mathbb{E}(\mathsf{ISR}_0\, \mathsf{ISR}_\Delta) = \rho \operatorname{var}(\mathsf{ISR}_0) + \mathsf{MISR}^2$$
$$= \rho\frac{\delta}{2-\delta} + \frac{\delta^2}{(1-\delta)^2}.$$

Letting $Q = \sqrt{\mathbb{E}(\mathsf{ISR}_0\, \mathsf{ISR}_\Delta)}$*, we can express the correlation coefficient as*

$$\rho = (\alpha-1)(Q + \mathsf{MISR})(Q - \mathsf{MISR}).$$

D. MD for Single-Tier Moving Networks

In single-tier MNs, the standard success probability, the conditional success probability, and the moments are denoted as $p_{\mathrm{s}}^{[v]}$, $P_{\mathrm{s}}^{[v]}$ and $M_b^{[v]}$ for general speeds v, respectively.

For the first moment of the conditional success probability M_1, we can take the expectation over the point process inside the integral in the (4). Since $\Phi(t)$ is a PPP for all t, the mobility of the BSs has no effect on the average SIR performance of the MNs. Hence $M_1^{[v]}$ does not depend on v, i.e., for all v,

$$M_1^{[v]} \equiv p_{\mathrm{s}}^{[0]}(\theta) = \frac{1}{{}_2F_1\left(1, -\delta; 1-\delta; -\theta\right)} = \frac{1}{\mathcal{F}_1(\theta)}. \quad (9)$$

where $\mathcal{F}_b(\theta) \triangleq {}_2F_1\left(b, -\delta; 1-\delta; -\theta\right),\ b \in \mathbb{C}$, and ${}_2F_1$ denotes the Gauss hypergeometric function.

To assess the benefits of mobility, we next analyze the moments of the conditional success probability, the variance of the conditional success probability, and the meta distribution of the SIR for the MNs in the extreme case $v \to \infty$ compared with the static case.

1) Static Case: In the static case, $\Phi(t) \equiv \Phi_0$. The b-th moments of the conditional success probability for SNs are known from [6] as

$$M_b^{[0]}(\theta) = \frac{1}{{}_2F_1\left(b, -\delta; 1-\delta; -\theta\right)} = \frac{1}{\mathcal{F}_b(\theta)},\ b \in \mathbb{C}. \quad (10)$$

The variance of the conditional success probability follows as

$$\operatorname{var} P_{\mathrm{s}}^{[0]}(\theta) = M_2 - M_1^2 = \frac{1}{\mathcal{F}_2(\theta)} - \frac{1}{\mathcal{F}_1^2(\theta)}. \quad (11)$$

2) High-Mobility Case: In the high-mobility case, we let $v \to \infty$ and thus the moving BSs follow an independent homogeneous PPP for each time t. The UEs connect to many different BSs within each time slot.

Proposition 1 (Moments for MNs in the high-mobility case) *The moments of the conditional success probability for MNs in the high-mobility case are given by*

$$M_b^{[\infty]}(\theta) = \frac{1}{\mathcal{F}_1^b(\theta)},\ b \in \mathbb{C}. \quad (12)$$

Proof: In the calculation of the conditional success probability $P_{\mathrm{s}}(\theta)$ in the high-mobility case, the expectations that involve the PPP and the fading are taken. The conditional success probability for MNs with high mobility is obtained as

$$\begin{aligned} P_{\mathrm{s}}^{[\infty]}(\theta) &= \int_0^1 \mathbb{P}(\mathrm{SIR}(t) > \theta \mid \Phi(t))\mathrm{d}t \\ &\overset{(a)}{=} \mathbb{E}_\Phi\left[\mathbb{P}(\mathrm{SIR}(t) > \theta \mid \Phi(t))\right] \\ &= \mathbb{P}\left(h > \theta r^\alpha \sum_{x\in\Phi\setminus\{x_0\}} h_x \|x\|^{-\alpha}\right) \\ &\overset{(b)}{=} \mathbb{E}_\Phi \prod_{x\in\Phi\setminus\{x_0\}} \frac{1}{1+\theta(\|x_0\|/\|x\|)^\alpha} \\ &\overset{(c)}{=} \frac{1}{{}_2F_1\left(1, -\delta; 1-\delta; -\theta\right)}, \end{aligned}$$

where (a) is due to the fact that by ergodicity, the time (the path) average equals the ensemble average, (b) is derived by averaging out the fading $h_i \sim \exp(1)$, and (c) follows from the pgfl of the PPP [34]. Hence $P_{\mathrm{s}}^{[\infty]}$ is deterministic, and $M_b^{[\infty]}(\theta)$ is simply its b-th power. It follows that as $v \to \infty$, the success probabilities for all the users become identical. ■

Combining (5) and (12), it can be seen that the meta distribution of the SIR for MNs does not depend on the transmission power and density of the moving BS.

The assumption $\lambda = 1$ means that for $v = 1$, the user essentially perceives two independent network realizations according to the conclusion from Sec. II-C. So we expect the variance to drop to about $1/2$ of its value in the static case. For $v = 2$, the user perceives 3 independent realizations, so the variance drops to $1/3$, etc. Thus, we can propose a tractable approximation of the variance for all speeds with the known $\operatorname{var} P_{\mathrm{s}}^{[0]}(\theta)$.

Approximation 1 (Approximation of the Variance) *A closed-form approximation of the variance of the conditional success probability for speed* v *is given by*

$$\operatorname{var} P_{\mathrm{s}}^{[v]} \simeq \frac{\operatorname{var} P_{\mathrm{s}}^{[0]}(\theta)}{1+v} = \frac{1}{1+v}\left(\frac{1}{\mathcal{F}_2(\theta)} - \frac{1}{\mathcal{F}_1^2(\theta)}\right). \quad (13)$$

The beta distribution with two parameters $M_1^{[v]}$ and $\operatorname{var} P_{\mathrm{s}}^{[v]}$ has been verified to be an effective approximation of the MD [6], [23], [27]. Since the exact variance for finite v seems hopeless to derive, we use the approximated variance in (13) to fit a beta distribution.

Approximation 2 (Beta Approximation) *The beta approximation of the MD for speed* v *is*

$$f(x) = \frac{x^{\frac{(\beta+1)-\mathcal{F}_1(\theta)}{\mathcal{F}_1(\theta)-1}}(1-x)^{\beta-1}}{B(\beta/(\mathcal{F}_1(\theta)-1), \beta)}, \quad (14)$$

where $B(\cdot)$ *is the beta function and* $\beta = \frac{\mathcal{F}_2(\theta)(1-\mathcal{F}_1(\theta))^2(v+1)}{\mathcal{F}_1(\theta)(\mathcal{F}_1(\theta)^2-\mathcal{F}_2(\theta))} + \frac{1}{\mathcal{F}_1(\theta)} - 1.$

This approximation is justified as follows. The beta probability density function (pdf) for a given value x is

$$f(x) = \frac{x^{\frac{\mu(\beta+1)-1}{1-\mu}}(1-x)^{\beta-1}}{B(\mu\beta/(1-\mu), \beta)}, \quad (15)$$

where $B(\cdot)$ is the beta function. The variance is given by

$$\sigma^2 \triangleq \operatorname{var} X = \frac{\mu(1-\mu)^2}{\beta+1-\mu}.$$

Matching the mean $\mu = M_1^{[v]}$ and approximated variance $\sigma^2 = \operatorname{var} P_s^{[v]}$, the approximated parameter of the beta distribution is derived as

$$\begin{aligned}\beta &= \frac{M_1^{[v]}\left(1-M_1^{[v]}\right)^2}{\operatorname{var} P_{\mathrm{s}}^{[v]}} - \left(1-M_1^{[v]}\right)\\ &\overset{(a)}{=} \frac{\mathcal{F}_2(\theta)(1-\mathcal{F}_1(\theta))^2(v+1)}{\mathcal{F}_1(\theta)(\mathcal{F}_1(\theta)^2-\mathcal{F}_2(\theta))} + \frac{1}{\mathcal{F}_1(\theta)} - 1, \end{aligned} \quad (16)$$

where (a) follows from substitutions based on the results from (9) and the approximated variance for speed v in (13). Based on $M_1^{[v]}$ and β, the beta approximation of the MD for speed v is given in (14).

In addition to the theoretical analysis of the special cases $v = 0$ and $v \to \infty$, simulations have been conducted for the intermediate range of speed v to demonstrate the accuracy of the approximation. Throughout the simulations in this section, without loss of generality, P and λ are set to 1 since the meta distribution is independent of the transmission power and density according to the results above. To simplify the simulation procedure, the averaging w.r.t. the Rayleigh fading is done analytically, i.e., the simulation is only used to average over the random geometry of the network. We produce 10000 PPP realizations of Φ_0, and then produce 40 time slots in the observation time interval $[0,1]$ for each chosen speed v. The nodes in each realization Φ_0 are set as the start points. The locations of nodes are updated in every time slot. We calculate the SIR of the typical user of in every time slot. The simulation results are obtained over the 10000×40 data points for each chosen v. Besides the figures of M_1 and variance, figures of the empirical MD for the static case and chosen maximum speed $v_{\max}$ are produced. The simulation parameters are: speed $v \in [0,\ v_{\max}]$, $v_{\max} = 50$, and SIR threshold $\theta = 3$ dB. For a path loss exponent of 4, the simulation region is $[0,16]^2$ with about 256 BSs, while for $\alpha = 3$, the simulation region is extended to $[0,40]^2$ with about 1600 BSs.

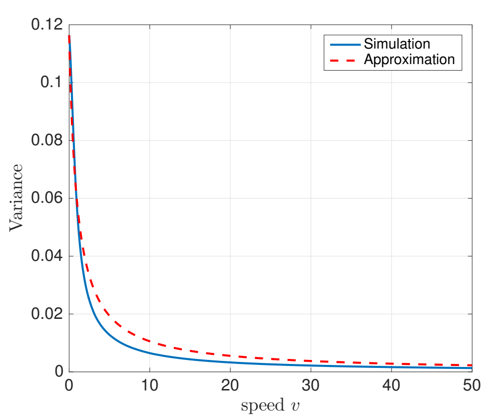

Fig. 2. Variance of $P_{\mathrm{s}}(\theta)$ with difference speeds v in MNs where $\lambda = 1$, $\alpha = 4$ and $\theta = 3$ dB.

Fig. 2 shows the simulated variance of the conditional success probability for networks with different speeds and its approximation. With the increasing mobility of the BSs, the variance is decreasing to 0. Shown as the dashed curve, the approximation provides an accurate fit to the simulation for all speeds v.

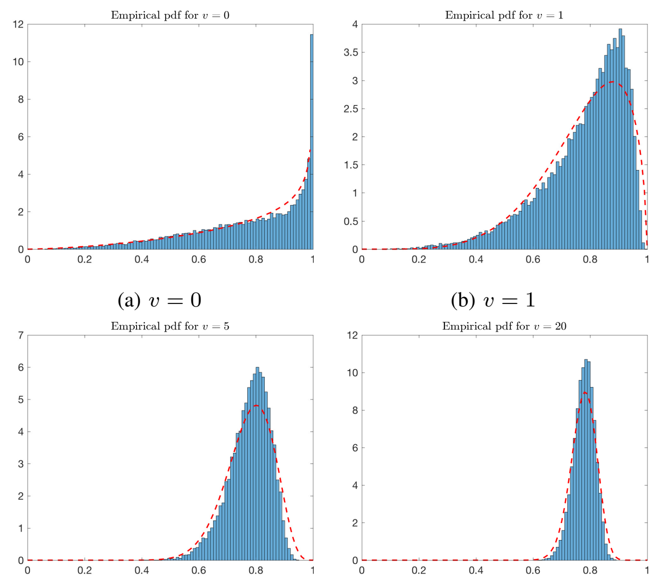

(a) $v = 0$ (b) $v = 1$ (c) $v = 5$ (d) $v = 20$

Fig. 3. Empirical pdf of the conditional success probability and its beta approximation (dashed curve) for $v = \{0, 1, 5, 20\}$ with $\theta = -5$ dB, where $\lambda = 1$ and $\alpha = 4$.

Fig. 3 show the empirical MD and its beta approximation (dashed curve) for the different speeds. These figures indicate how the distribution becomes more concentrated with increasing v. If $M_1 < 1/2$ (and small v), all beta distributions have positive skewness. However, the empirical distribution for $M_1 < 1/2$ with $v = 1$ or $v = 2$ shows (significant) negative skewness. In this case, the actual distribution can not be captured by the beta family of distribution. To obtain a more realistic mean success probability M_1, the SIR threshold is set to -5 dB in Fig. 3. For $M_1 > 1/2$, the skewness of the beta distribution is negative, and so is the skewness of the empirical distribution. It is notable that for $M_1 > 1/2$, the beta approximation from Approx. 2 gives a good fit to the meta distribution for all speeds.

E. Local Delay

The mean local delay M_{-1} is the -1-st moment of the conditional success probability [35]. It is defined as the mean number of transmission attempts before the first successful transmission if the transmitter is allowed to keep transmitting. In static Poisson cellular networks, the mean local delay has a phase transition at the critical value $\theta = 1/\delta - 1$, i.e., the mean local delay is finite when $\theta < 1/\delta - 1$ and infinite for $\theta \geq 1/\delta - 1$. An infinite mean local delay means that a significant fraction of UEs in the network suffers from high delay. The mean local delay of the typical UE for SNs follows as [6]

$$M_{-1}^{[0]}(\theta)=\frac{1-\delta}{1-\delta(1+\theta)},\ \theta<\frac{1}{\delta}-1. \tag{17}$$

Base on the (12), the mean local delay M_{-1} of the typical UE for MNs in the high-mobility case is given by

$$M_{-1}^{[\infty]}(\theta)=\mathcal{F}_1(\theta). \tag{18}$$

Based on the analysis of $M_{-1}(\theta)$, we conclude that in the high-mobility case, the mean local delay is simply $1/\mathbb{P}(\mathrm{SIR}>\theta)$; in the static case, conditioning on Φ, the -1-st moment of the conditional success probability is calculated, and the expectation w.r.t. the point process yields the local delay $\mathbb{E}_\Phi\left(1/\mathbb{P}(\mathrm{SIR}>\theta\mid\Phi)\right)$.

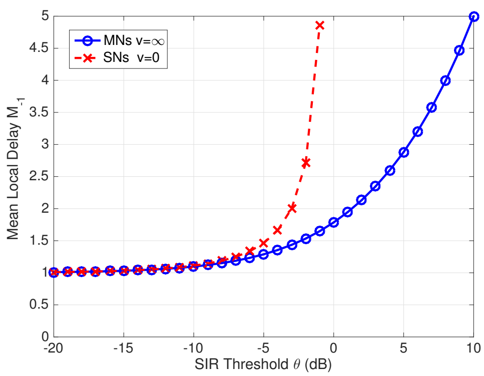

Fig. 4. Analytical results of mean local delay $M_{-1}(\theta)$ in two extreme cases of mobility $v=0,\,\infty$ where $\alpha=4$.

Fig. 4 shows the theoretical results for the mean local delay for $v=0$ and $v\to\infty$, and the critical value of phase transition θ in SNs can be observed. The mean local delay in MNs is finite and much smaller than in SNs especially when the SIR threshold θ approaches the critical value. The introduction of the moving BS can eliminate holes in the coverage of cellular SNs. Since every UE will be served by its passing moving BSs, mobility reduces the fraction of users with high delay.

III. Two-tier heterogeneous moving networks

A. System Model

Here, we consider a heterogeneous cellular network composed of two independent network tiers, namely a static macro BS tier (tier 1) and a moving BS tier (tier 2). According to the deployment in a dense urban scenario, tier 1 and tier 2 are accurately modeled by two independent homogeneous PPPs $\Phi_1(t)\equiv\Phi_1$ and $\Phi_2(t)$ with intensities of λ_1 and λ_2, respectively. Each BS in tier i ($i=1,2$) uses an identical transmission power P_i. All BSs are active at all times. The moving BS tier $\Phi_2(t)$ corresponds to single-tier MNs described in Sec. II. When $v=0$, this model reduces to a conventional heterogeneous cellular network (HCN) with two stationary tiers, i.e., a heterogeneous SN.

The 3GPP standardized channel propagation model for HCNs including distance-based path loss and Rayleigh fading is applied [36]. Based on evaluation assumptions in the 3GPP standard for HCNs [36], we let the path loss exponent of each tier be α and define $\delta\triangleq 2/\alpha$.

For a UE located at the origin, we define $T_i(t)$ to be the transmitter of the tier i that results in the strongest average received signal power at time t, i.e.,

$$T_i(t)\triangleq\arg\min_{x(t)\in\Phi_i(t)}\{\|x(t)\|\}. \tag{19}$$

The distance from the typical UE at the origin to the nearest transmitter in the i-th tier is denoted as $r_i(t)=\|T_i(t)\|$ at time t. Because the transmitters form an independent PPP at each time, $r_i(t)$ is a random variable with time-invariant pdf

$$f_{r_i(t)}(u)=2\pi\lambda_i u e^{-\pi\lambda_i u^2}. \tag{20}$$

We assume the open access strategy where the UEs are allowed to connect to any tier without restriction. Load balancing is taken into consideration by introducing a parameter called the range expansion bias β_i. The association scheme is based on the maximum biased-received-power (MBRP) $\beta_i P_i r_i(t)^{-\alpha}$. The positive biasing factor β_i implies that even for a lower received power from the i-th tier, UEs are biased to associate with tier i. Specifically, the typical UE is served by the i-th tier if and only if

$$\beta_i P_i r_i(t)^{-\alpha}>\beta_j P_j r_j(t)^{-\alpha},\quad j\neq i. \tag{21}$$

B. First Moment and Variance of the Conditional Success Probability for MNs

Here we analyze the moments of the conditional success probability as $v\to\infty$ and contrast it with the static case $v=0$.

The SIR of the typical UE assumed to be located at the origin and served by the i-th tier at time t can be written as

$$\mathrm{SIR}_i(t)=\frac{P_i h_{T_i(t)} r_i^{-\alpha}(t)}{\sum\limits_{k=1}^{2}\sum\limits_{x\in\Phi_k(t)\setminus\{T_i(t)\}}P_k h_x\|x\|^{-\alpha}}. \tag{22}$$

The ratios of density, transmission power, and bias factor determine the probability that the typical UE is associated with a particular tier and the SIR. We define

$$\hat{\lambda}\triangleq\frac{\lambda_2}{\lambda_1},\ \hat{P}\triangleq\frac{P_2}{P_1},\ \hat{B}\triangleq\frac{\beta_2}{\beta_1},\ G\triangleq\hat{\lambda}(\hat{P}\hat{B})^{\delta}. \tag{23}$$

Such parametrization is sensible since only the ratios of the densities, transmission powers, and bias factors matter.

It follows that, given $r_i(t)$, the conditional access probabilities that the typical UE associates with the i-th tier are

$$p_{(1)|r_1(t)}=e^{-\pi\lambda_2(\hat{P}\hat{B})^{\delta}r_1^2(t)}, \tag{24}$$

$$p_{(2)|r_2(t)}=e^{-\pi\lambda_1(\hat{P}\hat{B})^{-\delta}r_2^2(t)}. \tag{25}$$

The access probability that the typical UE associates with the i-th tier has been derived in [37, Lemma 1], which is here slightly reformulated as

$$p_{(1)}=\frac{1}{1+\hat{\lambda}(\hat{P}\hat{B})^{\delta}}=\frac{1}{1+G}, \tag{26}$$

$$p_{(2)}=\frac{1}{1+\hat{\lambda}^{-1}(\hat{P}\hat{B})^{-\delta}}=\frac{1}{1+G^{-1}}. \tag{27}$$

1) Static Case: In the case $v=0$, the conditional success probability is conditioned on the static tiers Φ_1 and Φ_2. The b-th moments and variance of the conditional success probability of the typical UE served by tier i and in the overall network are known from [27, Cor. 2] for Poisson two-tier cellular networks.

2) High-Mobility Case: In the case $v \to \infty$, due to the high mobility of the moving BSs in tier 2, the conditional success probability for two-tier heterogeneous MNs is obtained by averaging over the moving BS process $\Phi_2(t)$ in addition to the fading.

Given the static macro BS process and that the typical UE connects to tier i, the conditional success probability in the high-mobility case is given by

$$\begin{aligned} P_{\mathrm{s}|(i)}^{[\infty]}(\theta) &\triangleq \mathbb{P}(\mathrm{SIR}_i > \theta \mid \Phi_1) \\ &= \mathbb{P}\left(\frac{P_i h_{T_i(t)} r_i(t)^{-\alpha}}{\sum_{k=1}^{2} \sum_{x\in\Phi_k\setminus T_i(t)} P_k h_x \|x\|^{-\alpha}} > \theta \mid \Phi_1 \right) \\ &= \mathbb{P}\left(h_{T_i(t)} > \theta \sum_{k=1}^{2} \sum_{x\in\Phi_k\setminus T_i(t)} h_x \frac{P_k}{P_i} \frac{r_i^\alpha(t)}{\|x\|^\alpha} \mid \Phi_1 \right) \\ &\overset{(a)}{=} \mathbb{E}\left(e^{-\theta \sum_{k=1}^{2} \sum_{x\in\Phi_k\setminus T_i(t)} h_x \frac{P_k}{P_i} \frac{r_i^\alpha(t)}{\|x\|^\alpha}} \mid \Phi_1 \right), \end{aligned}$$

where (a) follows since $h_i \sim \exp(1)$. By averaging over the fading $h_x \sim \exp(1)$, the above expression is further developed for tier i $(i=1,2)$.

$$\begin{aligned} P_{\mathrm{s}|(1)}^{[\infty]}(\theta) &= \prod_{x\in\Phi_1\setminus T_1(t)} \frac{1}{1+\theta \frac{r_1^\alpha(t)}{\|x\|^\alpha}} \mathbb{E}_{\Phi_2} \prod_{x\in\Phi_2\setminus T_1(t)} \frac{1}{1+\theta \hat{P} \frac{r_1^\alpha(t)}{\|x\|^\alpha}} \\ &\overset{(a)}{=} e^{-\pi\lambda_2 \hat{P}^\delta \hat{B}^{\delta-1} \mu\theta {}_2F_1\left[1,1-\delta;2-\delta;-\theta\hat{B}^{-1}\right] r_1^2(t)} \\ &\quad \cdot \prod_{x\in\Phi_1\setminus T_1(t)} \frac{1}{1+\theta \frac{r_1^\alpha(t)}{\|x\|^\alpha}} \\ &\overset{(b)}{=} e^{-\pi\lambda_2 \hat{P}^\delta \hat{B}^\delta \left(\mathcal{F}_1\left(\frac{\theta}{\hat{B}}\right)-1\right) r_1^2(t)} \prod_{x\in\Phi_1\setminus T_1(t)} \frac{1}{1+\theta \frac{r_1^\alpha(t)}{\|x\|^\alpha}}, \end{aligned} \tag{28}$$

$$\begin{aligned} P_{\mathrm{s}|(2)}^{[\infty]}(\theta) &= \mathbb{E}_{\Phi_2} \prod_{x\in\Phi_1\setminus T_2(t)} \frac{1}{1+\frac{\theta}{\hat{P}} \frac{r_2^\alpha(t)}{\|x\|^\alpha}} \prod_{x\in\Phi_2\setminus T_2(t)} \frac{1}{1+\theta \frac{r_2^\alpha(t)}{\|x\|^\alpha}} \\ &\overset{(c)}{=} \mathbb{E}_{r_2(t)} \left[e^{-\pi\lambda_2\mu\theta {}_2F_1[1,1-\delta;2-\delta;-\theta] r_2^2(t)} \right. \\ &\quad \left. \cdot \prod_{x\in\Phi_1\setminus T_2(t)} \frac{1}{1+\theta\hat{P}^{-1} \frac{r_2^\alpha(t)}{\|x\|^\alpha}} \right] \\ &\overset{(d)}{=} \int_0^\infty e^{-\pi\lambda_2(\mathcal{F}_1(\theta)-1)r^2} \prod_{x\in\Phi_1\setminus T_2(t)} \frac{1}{1+\frac{\theta}{\hat{P}} \frac{r^\alpha}{\|x\|^\alpha}} f_{r_2(t)}(r)\mathrm{d}r \\ &= \mathbb{E}_{r_2(t)} \left[P_{\mathrm{s}|(2),r_2(t)}^{[\infty]} \right], \end{aligned} \tag{29}$$

where $P_{\mathrm{s}|(2),r_2(t)}^{[\infty]} = e^{-\pi\lambda_2(\mathcal{F}_1(\theta)-1)r_2^2(t)} \prod_{x\in\Phi_1\setminus T_2(t)} \frac{1}{1+\frac{\theta}{\hat{P}} \frac{r_2^\alpha(t)}{\|x\|^\alpha}}$, (a) and (c) follow from the PGFL of the PPP and the identity

$$ {}_2F_1(b,-\delta;1-\delta,-z) \equiv 1+\int_1^\infty \left(1-\left(1+z\frac{1}{t^{\frac{1}{\delta}}}\right)^{-b}\right)\mathrm{d}t, \tag{30}$$

(b) and (d) follow from the identity

$$\mathcal{F}_1(x) - 1 \equiv {}_2F_1[1,1-\delta;2-\delta;-x] \cdot x\mu, \tag{31}$$

where $\mu \triangleq \frac{\delta}{1-\delta}$.

The moments of the typical UE served by tier i $(i=1,2)$ follow as

$$M_{b,(1)}^{[\infty]} = \mathbb{E}_{\Phi_1}\left[p_{(1)|r_1(t)} \cdot P_{\mathrm{s}|(1)}^b(\theta)\right], \tag{32}$$

$$\begin{aligned} M_{b,(2)}^{[\infty]} &= p_{(2)}\mathbb{E}_{\Phi_1}\left[\left(P_{\mathrm{s}|(2)}^{[\infty]}(\theta)\right)^b\right] \\ &= p_{(2)}\mathbb{E}_{\Phi_1}\left[\left(\mathbb{E}_{r_2(t)}\left[P_{\mathrm{s}|(2),r_2(t)}^{[\infty]}(\theta)\right]\right)^b\right]. \end{aligned} \tag{33}$$

Conditioned on the typical UE served by the i-th tier, the b-th moments of the MD is denoted as $M_{b|(i)}$. The b-th moments of the conditional success probability for heterogenous MNs in the high-mobility case are

$$M_b^{[\infty]} = \sum_{k=1}^{2} M_{b,(k)}^{[\infty]} = p_{(1)} \cdot M_{b|(1)}^{[\infty]} + p_{(2)} \cdot M_{b|(2)}^{[\infty]}. \tag{34}$$

For the scenario that the UE nearby a bus/metro station connects to the a parked (stationary) bus/metro, we introduce the network modeling assumption that the serving BS from tier 2 is fixed. Given that the serving BS is at distance r_2, the moments corresponding to this conditional high-mobility case follow as

$$M_{b,(2)}^{\prime[\infty]} = \mathbb{E}_{\Phi_1}\left[p_{(2)|r_2(t)} \cdot \left(P_{\mathrm{s}|(2),r_2(t)}^{[\infty]}(\theta)\right)^b\right]. \tag{35}$$

Based on this modeling assumption above, we derive the tractable first moment and variance for MNs in the conditional high-mobility case.

Theorem 1 (The first moment for MNs with range expansion) *In the conditional high-mobility case, the first moment of the conditional success probabilities conditioned on tier i serving the typical user and for overall network of the heterogenous MN with range expansion are given by*

$$M_{1|(1)}^{[\infty]} = \frac{1+G}{\mathcal{F}_1(\theta) + G\mathcal{F}_1(\theta\hat{B}^{-1})}, \tag{36}$$

$$M_{1,(2)}^{\prime[\infty]} = \frac{1+G^{-1}}{\mathcal{F}_1(\theta) + G^{-1}\mathcal{F}_1(\theta\hat{B})}, \tag{37}$$

$$M_1^{\prime[\infty]} = \frac{1}{\mathcal{F}_1(\theta) + G\mathcal{F}_1(\frac{\theta}{\hat{B}})} + \frac{1}{\mathcal{F}_1(\theta) + \frac{\mathcal{F}_1(\theta\hat{B})}{G}}. \tag{38}$$

Proof: See Appendix A. ∎

Corollary 1 (The first moment for MNs without range expansion) *In the conditional high-mobility case, the first moments of the conditional success probabilities conditioned* *on tier i serving the typical user and for overall network with $\hat{P} = \hat{B} = 1$ are derived from Thm. 1 as*

$$M_{1|(1)}^{[\infty]} = M_{1|(2)}'^{[\infty]} = M_1'^{[\infty]} = \frac{1}{\mathcal{F}_1(\theta)}. \tag{39}$$

Proof: This can be easily obtained by setting $B = 1$ in (45). ■

Remark. *As shown in Thm. 1, it is remarkable that the standard success probabilities conditioned on tier i serving the typical user and for overall network in MNs with range expansion are the same as for SNs [27, Eq. (38)-(40)]. This shows that the mobility of the BSs does not improve the average success probability. The M_1s in single-tier MNs and multi-tier MNs without range expansion are the same, which implies that the multi-tier architecture does not improve the standard success probability.*

Theorem 2 (Variances for MNs with range expansion) *Given that the serving moving BS is fixed, the variances of the conditional success probabilities conditioned on tier i serving the typical user and for the overall network in the conditional high-mobility case are*

$$V_{|(1)}^{[\infty]} = \frac{1+G}{\mathcal{F}_2(\theta) + G\left(\mathcal{F}_1\left(\frac{\theta}{\hat{B}}\right) - 1\right)} - \left(\frac{1+G}{\mathcal{F}_1(\theta) + G\mathcal{F}_1\left(\frac{\theta}{\hat{B}}\right)}\right)^2, \tag{40}$$

$$V_{|(2)}'^{[\infty]} = \frac{1+G^{-1}}{\mathcal{F}_1(\theta) - 1 + \frac{\mathcal{F}_2(\theta\hat{B})}{G}} - \left(\frac{1+G^{-1}}{\mathcal{F}_1(\theta) + \frac{\mathcal{F}_1(\theta\hat{B})}{G}}\right)^2, \tag{41}$$

$$V'^{[\infty]} = \frac{1}{\mathcal{F}_2(\theta) + G\left(\mathcal{F}_1\left(\frac{\theta}{\hat{B}}\right) - 1\right)} + \frac{1}{\mathcal{F}_1(\theta) - 1 + \frac{\mathcal{F}_2(\theta\hat{B})}{G}} - \left(\frac{1}{\mathcal{F}_1(\theta) + G\mathcal{F}_1(\frac{\theta}{\hat{B}})} + \frac{1}{\mathcal{F}_1(\theta) + \frac{\mathcal{F}_1(\theta\hat{B})}{G}}\right)^2. \tag{42}$$

Proof: See Appendix B. ■

Corollary 2 (Variance for MNs without range expansion) *Given the serving BS from tier 2 is fixed, the variances of the conditional success probabilities conditioned on tier i serving the typical user and for overall network with $\hat{P} = \hat{B} = 1$ are*

$$V_{|(1)}^{[\infty]} = V_{|(2)}'^{[\infty]} = V'^{[\infty]} = \frac{1+\hat{\lambda}}{\mathcal{F}_2(\theta) + \hat{\lambda}\left(\mathcal{F}_1(\theta) - 1\right)} - \frac{1}{\mathcal{F}_1^2(\theta)}. \tag{43}$$

Proof: Follows directly from Thm. 2. ■

Remark. *As shown in Cor. 2, the variances for tier i and overall the network are the same when $\hat{P} = \hat{B} = 1$. The curves of both tiers and overall network coincide, which means the two tiers and overall network have the same* SIR *statistics, which are a function of the path loss exponent α, threshold θ, and density ratio $\hat{\lambda}$.*

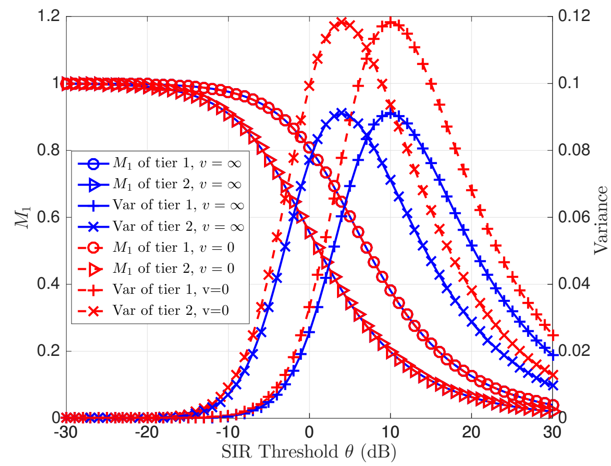

Fig. 5. M_1 and variance of tier i in MNs given the serving moving BS is fixed and SNs where $\alpha = 4$, $\hat{P} = 1/4$, $\hat{\lambda} = 100$, $\hat{B} = 6$ dB. Here, $p_{(1)} = 1\%, p_{(2)} = 99\%$.

Fig. 5 displays M_1 and the variance conditioned on tier i serving the typical user and for overall network in a two-tier heterogeneous MN with $v \to \infty$ and SN with $v = 0$, respectively. The curves of $M_1^{(i)}$ of tier i for MNs and SNs coincide. It can be seen that the (maximum) variance is lower in MNs than in SNs. The UEs, especially the cell-edge UEs that suffer from poor communication performance due to the long distance from all the fixed transmitters, will be served by their passing moving BSs sometimes due to the mobility of BSs. The moving BSs cover the holes in the coverage of conventional heterogeneous cellular networks and leads to a concentration in the per-user success probabilities, thereby increasing the fairness.

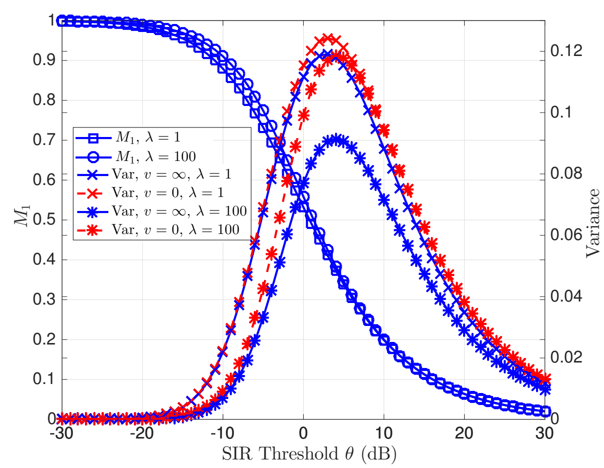

Fig. 6. $M_1^{[\infty]}$ and variance of overall network for MNs given the serving moving BS is fixed and SNs with $\hat{\lambda} = \{1, 100\}$, where $\alpha = 4$, $\hat{P} = 1/4$, $\hat{B} = 6$ dB. Here, $p_{(1)} = 50\%$, $p_{(2)} = 50\%$ when $\hat{\lambda} = 1$, $p_{(1)} = 1\%$, $p_{(2)} = 99\%$ when $\hat{\lambda} = 100$.

Simulations have been carried out with different ratios of moving BS and macro BS intensity, path loss exponents, and bias factors. M_1 and variance for the overall network in a two-tier heterogeneous MN given the serving moving BS is fixed and SN with different metrics are shown in Fig. 6, Fig. 7, and Fig. 8. In Fig. 6, it can be seen that for a bias factor ratio of 6 dB, the density ratio has a relatively small impact on the standard success probabilities. As the density of tier 2 increases, the variances of the overall network in both MNs and SNs decrease. A dense deployment of access points can help mitigate the variance while maintaining roughly the same M_1. Especially, increasing the number of moving BSs reduces the variance significantly compared to that of static BSs. With the tool of the MD, we can conclude that a dense deployment of moving BSs can bring some fairness benefits while maintaining the level of the standard success probability.

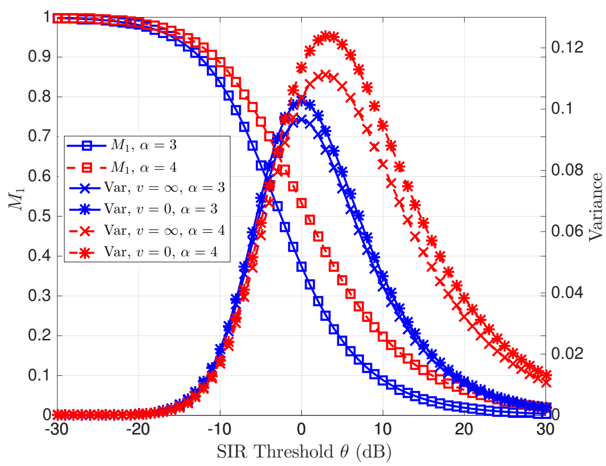

Fig. 7. $M_1^{[\infty]}$ and variance $M_2 - M_1^2$ of the overall network for MNs given the serving moving BS is fixed and SNs with path loss exponents $\alpha = \{3, 4\}$ where $\hat{\lambda} = 10$, $\hat{P} = 1/4$, $\hat{B} = 0$ dB.

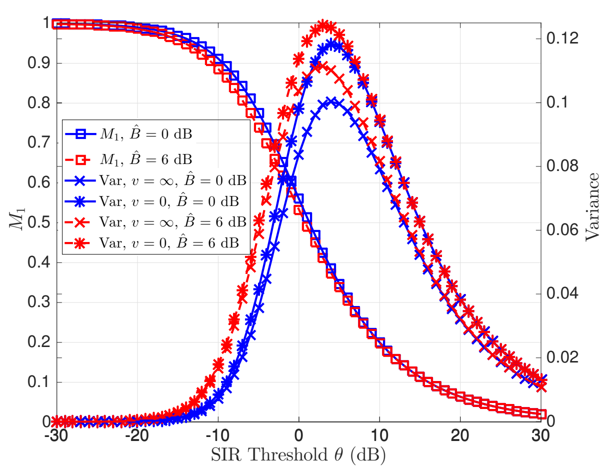

Fig. 8. $M_1^{[\infty]}$ and variance $M_2 - M_1^2$ of the overall network for MNs given the serving moving BS is fixed and SNs with bias factor ratios $\hat{B} = \{0, 6\}$ dB where $\hat{\lambda} = 10$, $\hat{P} = 1/4$, $\alpha = 4$.

As shown in Fig. 7, the simulation results for heterogeneous MNs in two extreme cases are almost the same as that for single-tier MNs. In heterogeneous MNs with large path loss, UEs have a higher standard success probability than MNs with small path loss while high-mobility BSs can decrease the higher variance. Since biasing means offloading, offloading from the macro BS tier to the moving BS tier will harm both the M_1 and variance of the entire network as shown in Fig. 8. The fairness enhancement brought by the mobility will narrow in MNs with range expansion.

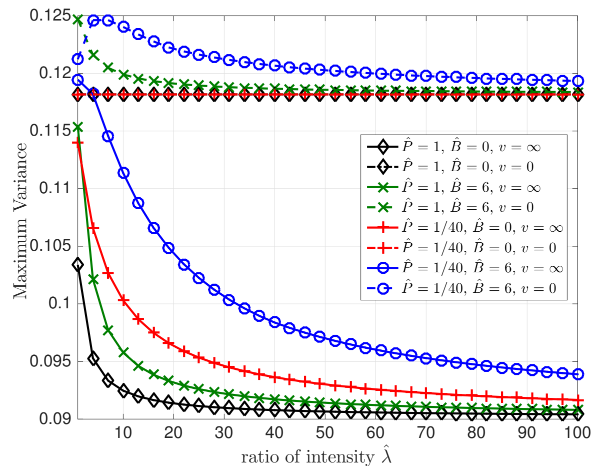

Fig. 9. Maximum variance $M_2 - M_1^2$ of the overall network for MNs given the serving moving BS is fixed and SNs with intensity ratios $\hat{\lambda}$ where $\alpha = 4$, $\hat{P} = \{1, 1/40\}$, $\hat{B} = 0$ dB.

As can be seen from Fig. 9, the maximum variance of the overall network for MNs given that the serving BS is at distance r_2 drops with the increasing of the intensity ratio $\hat{\lambda}$. Without range expansion, the maximum variance for SNs stays constant and is higher than for MNs. The decrease of the maximum variance will eventually slow down and stabilize when the intensity of moving BSs is much higher than that of macro BSs. The maximum variance of the MNs is lower than that of the SNs, and the gap will be wider with the increasing the ratio of intensity. Though the range expansion means offloading, larger range expansion biases will result in greater variances of success probability among the UEs. When the ratio of the moving BS and macro BS intensity is relatively small, the harm brought by offloading is more significant than the benefit brought by increasing the intensity of MRs.

IV. Conclusion

In this paper, the moving BSs are integrated in the conventional cellular network models, forming MNs in the heterogeneous 5G networks. To obtain fine-grained information on the SIR, we develop an SIR MD framework for the analysis of MNs. In MNs, the system model is described by stochastic geometry with a tractable mobility model. Firstly, the conditional success probability and MD for moving networks is defined. The conditional mean $\bar{\mathsf{ISR}}$ is defined and used to capture the correlation before and after the points of a PPP have been displaced. We derived the b-th moments of the conditional success probability for the single-tier MNs. With the b-th moments in hand, key performance metrics such as the exact MD, variance $M_1^2 - M_2$ and local delay can be calculated in closed-form. A closed-form approximation of the variance for general speeds is proposed. Using the approximated variance, we propose a beta approximation of the MD for general speeds. From the results, we can conclude that the variance goes to 0 as the speed of moving BSs $v \to \infty$. For intermediate speeds, simulations have been carried out to study the variance, local delay, and the meta distribution. The simulation results show that given an SIR threshold θ, the variance decreases sharply with increasing speed v and verify the accuracy of the proposed approximation of the variance. Moving BSs narrow the performance gap among UEs brought by large path loss exponent and high SIR threshold. For $M_1 > 1/2$, a beta approximation based on the approximated variance is valid for all speeds. The receiver in the single-tier MNs has a finite mean local delay that is much smaller than in SNs. It is notable that the variance with $v = \frac{1}{2\sqrt{\lambda}}$ is essentially the same as that with $v \to \infty$, namely 0.

The single-tier MN model is then extended to the two-tier heterogeneous MNs. Using the conditional success probability given the point process of moving BSs, the standard success probability and variance conditioned on tier i serving the typical user and for overall network are derived given that the serving moving BS is fixed. Simulations have been carried out with different ratios of moving BS and macro BS intensity, path loss exponents and bias factors. By increasing the intensity of moving BSs within certain range, the success probability gap among UEs can be narrowed down with the standard success probability remaining constant. When the transmission power of the moving BS is comparable to that of the macro BS, the fairness among the UEs will benefit more from the deployment of MNs. Although offloading from moving BSs to small cell BSs will widen the maximum variance among the UEs, the mobility of BSs results in lower variance among UEs in heterogeneous cellular networks.

Overall, the MD of the SIR in MNs extends the analytical framework for HCNs and offers new and interesting insights when the BSs are mobile. It helps assess the benefits of MNs and provides guidelines for the network optimization and design.

Appendix A
Proof of Theorem 1

In the conditional high-mobility case, the first moment of the conditional success probability of the typical UE served by the i-th $(i = 1, 2)$ tier is obtained as

$$
\begin{aligned}
M_{1,(1)}^{[\infty]} &= \mathbb{E}_{\Phi_1}\left[p_{(1)|r_1(t)} \cdot P_{\mathrm{s}|(1)}^{[\infty]}\right] \\
&\overset{(a)}{=} \mathbb{E}_{r_1(t)}\left[p_{(1)|r_1(t)} e^{-\left(\mathcal{F}_1(\theta)-1+G\left(\mathcal{F}_1\left(\frac{\theta}{\hat{B}}\right)-1\right)\right)\pi\lambda_1 r_1^2(t)}\right] \\
&\overset{(b)}{=} \int_0^\infty \exp\left(-u\left(\mathcal{F}_1(\theta)+G\mathcal{F}_1(\theta\hat{B}^{-1})\right)\right)\mathrm{d}u \\
&= \frac{1}{\mathcal{F}_1(\theta)+G\mathcal{F}_1(\theta\hat{B}^{-1})},
\end{aligned}
$$

$$
\begin{aligned}
M_{1,(2)}^{\prime[\infty]} &= \mathbb{E}_{\Phi_1}\left[\mathbb{E}_{r_2(t)}\left[p_{(2)|r_2(t)} \cdot P_{\mathrm{s}|(2),r_2(t)}^{[\infty]}\right]\right] \\
&= \mathbb{E}_{r_2(t)}\Bigg[p_{(2)|r_2(t)} e^{-\pi\lambda_2 r_2^2(t)(\mathcal{F}_1(\theta)-1)} \\
&\quad \cdot \mathbb{E}_{\Phi_1}\prod_{x\in\Phi_1\setminus T_2(t)} \frac{1}{1+\theta\hat{P}^{-1}\frac{r_2^\alpha(t)}{\|x\|^\alpha}}\Bigg] \\
&= \int_0^\infty e^{-\pi\lambda_1(\hat{P}\hat{B})^{-\delta}r_2^2(t)} e^{-\pi\lambda_2 r_2^2(t)\mathcal{F}_1(\theta)} \\
&\quad \cdot \mathbb{E}_{\Phi_1}\prod_{x\in\Phi_1\setminus T_2(t)} \frac{1}{1+\theta\hat{P}^{-1}\frac{r_2^\alpha(t)}{\|x\|^\alpha}} \mathrm{d}(\pi\lambda_2 r_2^2(t)) \\
&\overset{(c)}{=} \int_0^\infty e^{-\pi\lambda_2 r_2^2(t)\left(\mathcal{F}_1(\theta)+G^{-1}\mathcal{F}_1(\theta\hat{B})\right)} \mathrm{d}(\pi\lambda_2 r_2^2(t)) \\
&\overset{(d)}{=} \int_0^\infty \exp\left(-u\left(\mathcal{F}_1(\theta)+G^{-1}\mathcal{F}_1(\theta\hat{B})\right)\right)\mathrm{d}u \\
&= \frac{1}{\mathcal{F}_1(\theta)+G^{-1}\mathcal{F}_1(\theta\hat{B})},
\end{aligned}
$$

where (a) and (c) follow from the PGFL of PPP and the identify in (30). (b) and (d) are by using the substitution $u = \pi\lambda_i r_i^2(t)$.

Conditioned on the typical user associating with the i-th tier, the first moments of the conditional success probabilities in the conditional high-mobility case are given by

$$M_{1|(1)}^{[\infty]} = \frac{1+G}{\mathcal{F}_1(\theta)+G\mathcal{F}_1(\theta\hat{B}^{-1})}, \tag{44}$$

$$M_{1|(2)}^{\prime[\infty]} = \frac{1+G^{-1}}{\mathcal{F}_1(\theta)+G^{-1}\mathcal{F}_1(\theta\hat{B})}. \tag{45}$$

According to (34), the 1-st moment of the MD for the overall MNs can be obtained in (38).

Appendix B
Proof of Theorem 2

In the conditional high-mobility case, the variance of the conditional success probability given that the typical UE is served by tier i can be expressed as

$$V_{|(i)}^{\prime[\infty]} = \operatorname{var} P_{\mathrm{s}|(i)}^{[\infty]} = M_{2|(i)}^{[\infty]} - \left(M_{1|(i)}^{[\infty]}\right)^2. \tag{46}$$

Given the static macro BS, the second moment of the conditional success probability for the typical UE served by the tier 1 in the conditional high-mobility case is obtained as

$$
\begin{aligned}
M_{2,(1)}^{[\infty]} &= \mathbb{E}_{\Phi_1}\left[p_{(1)|r_1(t)} \cdot \left(P_{\mathrm{s}|(1)}^{[\infty]}\right)^2\right] \\
&= \mathbb{E}_{\Phi_1}\Bigg[p_{(1)|r_1(t)} e^{-2\pi\lambda_2\left(\hat{P}\hat{B}\right)^\delta\left(\mathcal{F}_1(\theta\hat{B}^{-1})-1\right)r_1^2(t)} \\
&\quad \cdot \prod_{x\in\Phi_1\setminus T_1(t)} \frac{1}{\left(1+\theta\|x\|^{-\alpha}r_1^\alpha(t)\right)^2}\Bigg] \\
&\overset{(a)}{=} \mathbb{E}_{r_1(t)}\Bigg[p_{(1)|r_1(t)} e^{-2\pi\lambda_2\left(\hat{P}\hat{B}\right)^\delta\left(\mathcal{F}_1\left(\theta\hat{B}^{-1}\right)-1\right)r_1^2(t)} \\
&\quad \cdot \int_{r_1(t)}^\infty 2\pi\lambda_1\left[1-\frac{1}{\left(1+\theta x_1^{-\alpha}r_1^\alpha(t)\right)^2}\right]x_1\mathrm{d}x_1\Bigg] \\
&\overset{(b)}{=} \int_0^\infty e^{-zG\left(\mathcal{F}_1\left(\frac{\theta}{\hat{B}}\right)-1\right)-z\left(1+\int_1^\infty\left(1-\frac{1}{\left(1+\theta u^{-\frac{\alpha}{2}}\right)^2}\right)\mathrm{d}u\right)}\mathrm{d}z
\end{aligned}
$$

$$\overset{(c)}{=} \int_0^\infty e^{-z\left(F_2(\theta)+G\left(\mathcal{F}_1\left(\theta\hat{B}^{-1}\right)-1\right)\right)}\mathrm{d}z$$
$$= \frac{1}{\mathcal{F}_2(\theta)+G\left(\mathcal{F}_1\left(\theta\hat{B}^{-1}\right)-1\right)}, \tag{47}$$

Given the static macro BS and that the serving BS is fixed, the second moment of the conditional success probability for the typical UE served by the tier 2 in the conditional high-mobility case is obtained as

$$\begin{aligned} M'^{[\infty]}_{2,(2)} &= \mathbb{E}_{\Phi_1}\left[\mathbb{E}_{r_2(t)}\left[p_{(2)|r_2(t)}\cdot\left(P^{[\infty]}_{\mathrm{s}|(2),r_2(t)}\right)^2\right]\right] \\ &= \mathbb{E}_{r_2(t)}\left[p_{(2)|r_2(t)}e^{-2\pi\lambda_2 r_2^2(t)(\mathcal{F}_1(\theta)-1)}\right. \\ &\quad \left.\cdot\,\mathbb{E}_{\Phi_1}\prod_{x\in\Phi_1\setminus T_2(t)}\frac{1}{\left(1+\theta\hat{P}^{-1}\frac{r_2^\alpha(t)}{\|x\|^\alpha}\right)^2}\right] \\ &\overset{(d)}{=} \int_0^\infty e^{-\pi\lambda_2 r^2(G^{-1}+\mathcal{F}_1(\theta)-1)} \\ &\quad \cdot\, e^{\int_r^\infty -2\pi\lambda_1\left[1-\frac{1}{\left(1+\theta\hat{P}^{-1}x_1^{-\alpha}r^\alpha\right)^2}\right]x_1\mathrm{d}x_1}\,\mathrm{d}(\pi\lambda_2 r^2) \\ &\overset{(e)}{=} \int_0^\infty e^{-u(\mathcal{F}_1(\theta)-1)-\frac{u}{G}\left(1+\int_1^\infty\left[1-\frac{1}{\left(1+\frac{\theta}{\hat{B}}t^{-\frac{1}{\delta}}\right)^2}\right]\mathrm{d}t\right)}\mathrm{d}u \\ &\overset{(f)}{=} \int_0^\infty e^{-u\left(\mathcal{F}_1(\theta)-1+G^{-1}\mathcal{F}_2\left(\theta\hat{B}\right)\right)}\mathrm{d}u \\ &= \frac{1}{\mathcal{F}_1(\theta)-1+G^{-1}\mathcal{F}_2\left(\theta\hat{B}\right)}, \end{aligned} \tag{48}$$

where (a) and (d) follow from the PGFL of the PPP, (b) is by using the substitution $u=\frac{x_1^2}{r_1^2(t)}$, (e) is by using the variable substitution $t=(\hat{P}\hat{B})^{\frac{1}{\delta}}x_1^2 r^{-2}$ and $z=\pi\lambda_2 r^2$, (c) and (f) follow from the identity (30).

Conditioned on the typical UE connecting to the i-th tier, the second moments of the conditional success probability given that the serving BS is fixed are

$$M^{[\infty]}_{2|(1)} = \frac{1+G}{\mathcal{F}_2(\theta)+G\left(\mathcal{F}_1\left(\theta\hat{B}^{-1}\right)-1\right)}, \tag{49}$$

$$M'^{[\infty]}_{2|(2)} = \frac{1+G^{-1}}{\mathcal{F}_1(\theta)-1+G^{-1}\mathcal{F}_2\left(\theta\hat{B}\right)}. \tag{50}$$

According to the definition of the variance in (46), the variances of the conditional success probabilities for each tier in the conditional high-mobility case can be obtained based on the known first and second moments for each tier.

REFERENCES

[1] Cisco, "Cisco Visual Networking Index: Global Mobile Data Traffic Forecast Update 2010-2015," *Cisco white paper*, Feb. 2011.

[2] *Study on Enhancement of 3GPP Support for 5G V2X Services*, 3rd Generation Partnership Project (3GPP), Technical Specification (TS) V16.1.1, Sep. 2018.

[3] M. Haenggi, J. G. Andrews, F. Baccelli, O. Dousse, and M. Franceschetti, "Stochastic geometry and random graphs for the analysis and design of wireless networks," *IEEE Journal on Selected Areas in Communications*, vol. 27, no. 7, pp. 1029–1046, Sep. 2009.

[4] A. Guo and M. Haenggi, "Spatial stochastic models and metrics for the structure of base stations in cellular networks," *IEEE Transactions on Wireless Communications*, vol. 12, no. 11, pp. 5800–5812, Nov. 2013.

[5] B. Błaszczyszyn, M. Haenggi, P. Keeler, and S. Mukherjee, *Stochastic geometry analysis of cellular networks*. Cambridge University Press, 2018.

[6] M. Haenggi, "The meta distribution of the SIR in Poisson bipolar and cellular networks," *IEEE Transactions on Wireless Communications*, vol. 15, no. 4, pp. 2577–2589, Apr. 2016.

[7] Y. Sui, J. Vihriala, A. Papadogiannis, M. Sternad, W. Yang, and T. Svensson, "Moving cells: a promising solution to boost performance for vehicular users," *IEEE Communications Magazine*, vol. 51, no. 6, pp. 62–68, Jun. 2013.

[8] E. Tanghe, W. Joseph, L. Verloock, and L. Martens, "Evaluation of vehicle penetration loss at wireless communication frequencies," *IEEE Transactions on Vehicular Technology*, vol. 57, no. 4, pp. 2036–2041, Jul. 2008.

[9] Y. Sui, A. Papadogiannis, and T. Svensson, "The potential of moving relays – a performance analysis," in *IEEE Vehicular Technology Conference (VTC Spring)*, Yokohama, May 2012, pp. 1–5.

[10] Y. Sui, A. Papadogiannis, W. Yang, and T. Svensson, "Performance comparison of fixed and moving relays under co-channel interference," in *IEEE Global Communications Conference Workshops*, Anaheim, CA, Dec. 2012, pp. 574–579.

[11] A. Khan and A. Jamalipour, "Moving relays in heterogeneous cellular networks – a coverage performance analysis," *IEEE Transactions on Vehicular Technology*, vol. 65, no. 8, pp. 6128–6135, Aug. 2016.

[12] X. Xu, Z. Sun, X. Dai, T. Svensson, and X. Tao, "Modeling and analyzing the cross-tier handover in heterogeneous networks," *IEEE Transactions on Wireless Communications*, vol. 16, no. 12, pp. 7859–7869, Dec. 2017.

[13] Z. Tong and M. Haenggi, "Throughput analysis for full-duplex wireless networks with imperfect self-interference cancellation," *IEEE Transactions on Communications*, vol. 63, no. 11, pp. 4490–4500, Nov. 2015.

[14] G. Nigam, P. Minero, and M. Haenggi, "Coordinated multipoint joint transmission in heterogeneous networks," *IEEE Transactions on Communications*, vol. 62, no. 11, pp. 4134–4146, Nov. 2014.

[15] X. Xu, Y. Zhang, and X. Tao, "Coverage analysis for moving relay enabled cellular networks," *Electronics Letters*, vol. 52, no. 20, pp. 1727–1729, Sep. 2016.

[16] Y. Chen, P. Martins, L. Decreusefond, F. Yan, and X. Lagrange, "Stochastic analysis of a cellular network with mobile relays," in *IEEE Global Communications Conference*, Austin, TX, Dec. 2014, pp. 4758–4763.

[17] X. Tang, X. Xu, T. Svensson, and X. Tao, "Coverage performance of joint transmission for moving relay enabled cellular networks in dense urban scenarios," *IEEE Access*, vol. 5, pp. 13 001–13 009, Jul. 2017.

[18] Z. Gong and M. Haenggi, "The local delay in mobile Poisson networks," *IEEE Transactions on Wireless Communications*, vol. 12, no. 9, pp. 4766–4777, Sep. 2013.

[19] Z. Gong and M. Haenggi, "Interference and outage in mobile random networks: Expectation, distribution, and correlation," *IEEE Transactions on Mobile Computing*, vol. 13, no. 2, pp. 337–349, Feb. 2014.

[20] S. Guruacharya and E. Hossain, "Approximation of meta distribution and its moments for Poisson cellular networks," *IEEE Wireless Communications Letters*, vol. 7, no. 6, pp. 1074–1077, Dec. 2018.

[21] M. Haenggi, "Efficient calculation of meta distributions and the performance of user percentiles," *IEEE Wireless Communications Letters*, vol. 7, no. 6, pp. 982–985, Dec. 2018.

[22] N. Deng and M. Haenggi, "A fine-grained analysis of millimeter-wave device-to-device networks," *IEEE Transactions on Communications*, vol. 65, no. 11, pp. 4940–4954, Nov. 2017.

[23] Y. Wang, M. Haenggi, and Z. Tan, "The meta distribution of the SIR for cellular networks with power control," *IEEE Transactions on Communications*, vol. 66, no. 4, pp. 1745–1757, Apr. 2018.

[24] J. Tang, G. Chen, and J. P. Coon, "The meta distribution of the secrecy rate in the presence of randomly located eavesdroppers," *IEEE Wireless Communications Letters*, vol. 7, no. 4, pp. 630–633, Aug. 2018.

[25] Y. Wang, Q. Cui, M. Haenggi, and Z. Tan, "On the SIR meta distribution for Poisson networks with interference cancellation," *IEEE Wireless Communications Letters*, vol. 7, no. 1, pp. 26–29, Feb. 2018.

[26] M. Salehi, A. Mohammadi, and M. Haenggi, “Analysis of D2D underlaid cellular networks: SIR meta distribution and mean local delay,” *IEEE Transactions on Communications*, vol. 65, no. 7, pp. 2904–2916, Jul. 2017.

[27] Y. Wang, M. Haenggi, and Z. Tan, “SIR meta distribution of K-tier downlink heterogeneous cellular networks with cell range expansion,” *IEEE Transactions on Communications*, vol. 67, no. 4, pp. 3069–3081, Apr. 2019.

[28] S. S. Kalamkar and M. Haenggi, “Simple approximations of the SIR meta distribution in general cellular networks,” *IEEE Transactions on Communications*, vol. 67, no. 6, pp. 4393–4406, Jun. 2019.

[29] M. Salehi, H. Tabassum, and E. Hossain, “Meta distribution of SIR in large-scale uplink and downlink NOMA networks,” *IEEE Transactions on Communications*, vol. 67, no. 4, pp. 3009–3025, Apr. 2019.

[30] H. S. Dhillon, R. K. Ganti, F. Baccelli, and J. G. Andrews, “Modeling and analysis of K-tier downlink heterogeneous cellular networks,” *IEEE Journal on Selected Areas in Communications*, vol. 30, no. 3, pp. 550–560, Apr. 2012.

[31] J. Gil-Pelaez, “Note on the inversion theorem,” *Biometrika*, vol. 38, no. 3-4, pp. 481–482, Dec. 1951.

[32] M. Haenggi, “The mean interference-to-signal ratio and its key role in cellular and amorphous networks,” *IEEE Wireless Communications Letters*, vol. 3, no. 6, pp. 597–600, Dec. 2014.

[33] R. K. Ganti and M. Haenggi, “Asymptotics and approximation of the SIR distribution in general cellular networks,” *IEEE Transactions on Wireless Communications*, vol. 15, no. 3, pp. 2130–2143, Mar. 2016.

[34] M. Haenggi, *Stochastic geometry for wireless networks*. Cambridge, UK: Cambridge University Press, 2012.

[35] ——, “The local delay in Poisson networks,” *IEEE Transactions on Information Theory*, vol. 59, no. 3, pp. 1788–1802, Mar. 2013.

[36] *Evolved Universal Terrestrial Radio Access (E-UTRA); Further Advancements for E-UTRA Physical Layer Aspects*, 3rd Generation Partnership Project (3GPP), Technical Report (TR) V 11.1.0, Jan. 2013.

[37] H. S. Jo, Y. J. Sang, P. Xia, and J. G. Andrews, “Heterogeneous cellular networks with flexible cell association: A comprehensive downlink SINR analysis,” *IEEE Transactions on Wireless Communications*, vol. 11, no. 10, pp. 3484–3495, Oct. 2012.

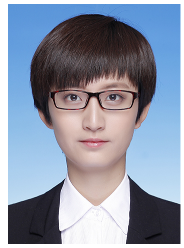

Xiaoxuan Tang received her B.S. degree in information and communication engineering from the Central South University (CSU) in 2010. She received her PH.D. degree in Information and Communication Engineering from the Beijing University of Posts and Telecommunications (BUPT) in 2019. Meanwhile, she was a Visiting Ph.D Student in Prof. Martin Haenggi’s Group at the University of Notre Dame, Notre Dame, IN, USA, from 2017 to 2018. Currently, she is a standard engineer in the China Mobile Research Institute (CMRI). Her research interests are in the area of wireless communication, including direction of moving’ networks and stochastic geometry.

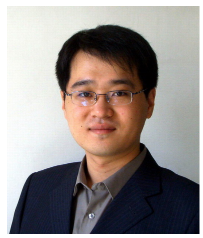

Xiaodong Xu (S’06-M’07-SM’18) received his B.S degree in Information and Communication Engineering and Master’s Degree in Communication and Information System both from Shandong University in 2001 and 2004 separately. He received his Ph.D. degrees of Circuit and System in Beijing University of Posts and Telecommunications (BUPT) in 2007. He is currently a professor of BUPT. He has coauthored nine books and more than 120 journal and conference papers. He is also the inventor or co-inventor of 39 granted patents. His research interests cover moving networks, mobile edge computing, caching and massive machine-type communications. He is an Associate Editor of IEEE ACCESS.

Martin Haenggi (S’95-M’99-SM’04-F’14) received the Dipl.-Ing. (M.Sc.) and Dr.sc.techn. (Ph.D.) degrees in electrical engineering from the Swiss Federal Institute of Technology in Zurich (ETH) in 1995 and 1999, respectively. Currently he is the Freimann Professor of Electrical Engineering and a Concurrent Professor of Applied and Computational Mathematics and Statistics at the University of Notre Dame, Indiana, USA. In 2007-2008, he was a visiting professor at the University of California at San Diego, and in 2014-2015 he was an Invited Professor at EPFL, Switzerland. He is a co-author of the monographs “Interference in Large Wireless Networks” (NOW Publishers, 2009) and “Stochastic Geometry Analysis of Cellular Networks” (Cambridge University Press, 2018) and the author of the textbook “Stochastic Geometry for Wireless Networks” (Cambridge, 2012), and he published 15 single-author journal articles. His scientific interests lie in networking and wireless communications, with an emphasis on cellular, amorphous, ad hoc (including D2D and M2M), cognitive, and vehicular networks. He served as an Associate Editor of the Elsevier Journal of Ad Hoc Networks, the IEEE Transactions on Mobile Computing (TMC), the ACM Transactions on Sensor Networks, as a Guest Editor for the IEEE Journal on Selected Areas in Communications, the IEEE Transactions on Vehicular Technology, and the EURASIP Journal on Wireless Communications and Networking, as a Steering Committee member of the TMC, and as the Chair of the Executive Editorial Committee of the IEEE Transactions on Wireless Communications (TWC). From 2017 to 2018, he was the Editor-in-Chief of the TWC. Currently he is an editor for MDPI Information. For both his M.Sc. and Ph.D. theses, he was awarded the ETH medal. He also received a CAREER award from the U.S. National Science Foundation in 2005 and three awards from the IEEE Communications Society, the 2010 Best Tutorial Paper award, the 2017 Stephen O. Rice Prize paper award, and the 2017 Best Survey paper award, and he is a Clarivate Analytics Highly Cited Researcher.